2012

Electric Field Exposure Triggers and Guides Formation of Pseudopod-Like Blebs in U937 Monocytes

Mikhail A. Rassokhin
Old Dominion University

Andrei G. Pakhomov
Old Dominion University

Original Publication Citation

Rassokhin, M. A., & Pakhomov, A. G. (2012). Electric field exposure triggers and guides formation of pseudopod-like blebs in U937 monocytes. *Journal of Membrane Biology, 245*(9), 521-529. doi:10.1007/s00232-012-9433-7

Published in final edited form as:
J Membr Biol. 2012 September ; 245(9): 521–529. doi:10.1007/s00232-012-9433-7.

Electric Field Exposure Triggers and Guides Formation of Pseudopod-Like Blebs in U937 Monocytes

Mikhail A. Rassokhin and **Andrei G. Pakhomov**
Frank Reidy Research Center for Bioelectrics, Old Dominion University, 4211 Monarch Way, Suite 300, Norfolk, VA 23508, USA

Mikhail A. Rassokhin: mrass002@odu.edu

Abstract

We describe a new phenomenon of anodotropic pseudopod-like blebbing in U937 cells stimulated by nanosecond pulsed electric field (nsPEF). In contrast to “regular,” round-shaped blebs, which are often seen in response to cell damage, pseudopod-like blebs (PLBs) formed as longitudinal membrane protrusions toward anode. PLB length could exceed the cell diameter in 2 min of exposure to 60-ns, 10-kV/cm pulses delivered at 10–20 Hz. Both PLBs and round-shaped nsPEF-induced blebs could be efficiently inhibited by partial isosmotic replacement of bath NaCl for a larger solute (sucrose), thereby pointing to the colloid-osmotic water uptake as the principal driving force for bleb formation. In contrast to round-shaped blebs, PLBs retracted within several minutes after exposure. Cells treated with 1 nM of the actin polymerization blocker cytochalasin D were unable to form PLBs and instead produced stationary, spherical blebs with no elongation or retraction capacity. Live cell fluorescent actin tagging showed that during elongation actin promptly entered the PLB interior, forming bleb cortex and scaffold, which was not seen in stationary blebs. Overall, PLB formation was governed by both passive (physicochemical) effects of membrane permeabilization and active cytoskeleton assembly in the living cell. To a certain extent, PLB mimics the membrane extension in the process of cell migration and can be employed as a nonchemical model for studies of cytomechanics, membrane–cytoskeleton interaction and cell motility.

Keywords

Electroporation; Nanosecond pulsed electric field; Colloid-osmotic swelling; Blebbing; Membrane protrusion; Cell motility

Introduction

Permeabilization of the cellular membrane by pulsed electric field, including nanosecond pulsed electric field (nsPEF), triggers cell reshaping due to swelling and blebbing (Gass and Chernomordik 1990; Deng et al. 2003; André et al. 2010). Intact cells maintain osmotic equilibrium with extracellular buffer (Hoffmann et al. 2009), but electropermeabilized cells are unable to do that effectively. Swelling in such cells is caused by a colloid-osmotic mechanism (Kinosita and Tsong 1977; Saulis 1999; Pakhomov and Pakhomova 2010) that results from differential permeability of the electroporated membrane to extra-and intracellular solutes. In brief, pores formed in the cell membrane due to pulse application are permeable to small ions but not to larger molecules. Bath buffer contains predominantly

Correspondence to: Mikhail A. Rassokhin, mrass002@odu.edumedchel@gmail.com.

small ions and molecules, while the cellular interior contains a fraction of large organic molecules and anions. After permeabilization, small ions like Na^+ and Cl^- enter the cell down their electrochemical gradients. Meanwhile, large pore-impermeant organic molecules and anions remain trapped inside. Osmolality created by organic molecules and entering ions becomes larger than osmolality of the bath buffer, which remains undisturbed due to its large volume. Such a mechanism generates osmotic gradient and drives water uptake.

Swelling in nsPEF-treated cells is often accompanied by formation of blebs, rounded membrane protrusions that appear on the cell surface in an apparently uncontrolled manner (Tekle et al. 2008; Pakhomov et al. 2009). Currently, the mechanisms and implementations of blebbing for physiology of electroporated cells are not clear. Supposedly, blebbing is a by-product of PEF-induced cell damage (Tsong 1991); however, outside the research area of electroporation, blebbing is commonly seen in the life cycle of intact cells (Blaser et al. 2006). Such blebs form during cytokinesis (Tinevez et al. 2009), migration (Charras and Paluch 2008), in attaching cells (Bereiter-Hahn et al. 1990) and in response to physiological stimuli (Torgerson and McNiven 1998).

In early studies, blebs were described as “clear, round cytoplasmic protrusions” (Hogue 1919) and referred to as blisters (Zollinger 1948) or bubbles (Holtfreter 1944). At present, the term “blebbing” is also used to describe membrane evaginations during cell spreading (Norman et al. 2011) and cell division (Pletjushkina et al. 2001), as well as in necrotic (Barros et al. 2003) and apoptotic (Sebbagh et al. 2001) cell damage. “Membrane ballooning” is another term that illustrates terminal blebbing in necrotic cells (Petersen and Dailey 2004; Lang et al. 2011). Due to the lack of clear definition and classification, the term “bleb” may be confusing when used outside the context of physiological or pathological processes. In this article we will differentiate between reversible, nonlethal blebbing and stationary blebbing, which is a sign of cell damage (Fackler and Grosse 2008).

Modern knowledge about blebbing and its mechanisms comes from multiple sources. Reversible blebs and their life cycle were comprehensively studied in cell lines with defects in actin polymerization. Such cells exhibit intense and reversible blebbing due to weakening of membrane–cytoskeleton adhesion (Cunningham et al. 1992; Derivery et al. 2008). Another factor responsible for bleb formation is actomyosin contractility of cell cortex and resulting increase in cortical tension (Dai and Sheetz 1999). In general, bleb formation can also be triggered by local transmembrane ion transport and associated water uptake (Mitchison et al. 2008). As mentioned previously, in electropermeabilized cells the colloid-osmotic water uptake also results from increased inward ion transport (Pakhomov and Pakhomova 2010). Hence, blebs induced by nsPEF may not only resemble regular blebs morphologically but also form through similar mechanisms.

Reversible and stationary blebs nucleate on the cell surface and inflate while remaining attached to the cell body through the neck region. Expansion of blebs lasts several seconds or minutes and results in the formation of rounded, membrane-bound protrusions, the size of which may become comparable to the size of the cell body. At the early stage of formation, morphological distinctions between reversible and stationary blebs are negligible. Both bleb types are present as transparent, membrane-bound, rounded protrusions with no cytoskeleton or organelles (Cunningham 1995). However, upon maturation the interior of reversible blebs becomes filled with de novo forming actin fibrils (Charras et al. 2006) that participate in the organization of contractile bleb cortex. Cortex assembly is associated with reestablishment of membrane–cytoskeleton integrity and further bleb retraction. Cortex contractility in reversible blebs is attributed to the presence of actomyosin motors (Charras et al. 2005). In contrast, formation of actin scaffold or contractile cortex does not occur in stationary blebs

formed during necrosis (Barros et al. 2003) or due to cytoskeletal toxin exposure (Charras 2008). Once inflation in such blebs stops, they remain stagnant and show no retraction.

Reversible blebbing passes through cycles of membrane expansion, reassembly of cortical cytoskeleton and retraction due to actomyosin contractility (Charras et al. 2006). Such a mechanism of membrane expansion may provide an alternative to actin-driven protrusion formation for cell locomotion (Keller and Eggli 1998; Maugis et al. 2010). In several works blebbing already has been established as a mechanism of cell migration (Fackler and Grosse 2008).

Typical blebs formed due to nsPEF exposure are stationary and reflect either apoptotic or necrotic cell transformation. However, we found an all new type of blebs that we called “pseudopod-like blebs” (PLBs). PLBs are characterized by elongated shape, fast directional growth toward anode and rapid retraction following nsPEF exposure. Some of these findings were reported previously in meeting proceedings (Rassokhin and Pakhomov 2010, 2011). This is the first systematic study of some PLB properties and the mechanisms that underlie their formation.

Materials and Methods

Cell Line and Propagation

This study was entirely performed on human suspension promonocytic U937 cells that were obtained from the ATCC (Mannanas, VA). Cells were propagated at 37 °C with 5 % CO_2 in air. In accordance with the supplier’s recommendations, cells were maintained in RPMI 1640 growth medium containing L-glutamine and supplemented with 10 % fetal bovine serum and 1 % penicillin/streptomycin. Cell culture components were obtained from Atlanta Biologicals (Norcross, GA) or Mediatech Cellgro (Herndon, VA). Before the experiment, cells were transferred onto glass coverslips pretreated with poly-L-lysine (Sigma-Aldrich, St. Louis, MO). Cells were left in full growth medium for at least 30 min prior to experiments.

Cell Imaging and Image Analysis

For timelapse image recording a coverslip with attached cells was placed into a glass-bottomed chamber (Warner Instruments, Hamden, CT) mounted on an IX81 motorized inverted microscope (Olympus, Center Valley, PA). Differential-interference contrast (DIC) and fluorescence imaging was performed using a 40 × dry objective (NA0.95) or a 60 × oil objective (NA 1.42). Cell images were recorded using the FV 1000 confocal laser scanning system (Olympus).

Cell images were taken at regular intervals of 4–5 s. Typically, six or seven images were captured prior to exposure. nsPEF treatment started 30 s into the experiment and continued for 30, 60 or 120 s. All experiments were performed at room temperature.

DIC images were analyzed for blebbing probability, location and bleb size. PLBs were defined as longitudinal, anodotropic blebs with the length exceeding at least one cell diameter. For measurement of membrane permeability a fluorescent membrane integrity marker, propidium iodide (Sigma-Aldrich), was added to the exposure buffer at a concentration of 5 μg/ml (~7.5 μM). To avoid saturation of the fluorescent channel, the sensitivity of the detector was calibrated on cells permeabilized with 0.3 % digitonin (Sigma-Aldrich). In other experiments to visualize actin rearrangements caused by nsPEF, rhodamine-phalloidin conjugate (Cytoskeleton, Denver, CO) was added to the bath buffer at a concentration of 28 nM. Analyses of blebbing, propidium uptake and actin rearrangements were performed using MetaMorph 7.7 software (Molecular Devices, Sunnyvale, CA).

Experimental Chemicals and Buffers

All experiments, except with sucrose, were performed in a bath buffer that contained (in mM) 135 NaCl, 5 KCl, 4 $MgCl_2$, 3 HEPES, 2 Na-EGTA and 10 glucose at pH 7.4 (Nesin et al. 2011). In experiments on the verification of the colloid-osmotic mechanism, we replaced 22.5, 45 or 90 mM of NaCl with isosmotic amounts of sucrose (45, 90 and 180 mM, respectively). The final osmolality of all experimental buffers remained at ~290 mOsm/kg, as measured with a freezing point micro-osmometer (Advanced Instruments, Norwood, MA). Chemicals were purchased from Sigma-Aldrich unless stated overwise. Rhodamine-phalloidin (Cytoskeleton) was dissolved in 100 % methanol, while cytochalasin D was dissolved in 100 % DMSO. In experiments studying actin rearrangements, vehicle (0.001 % DMSO) was used as a negative control. Overall exposure of cells to cytochalasin D before image recording was kept to a minimum and did not exceed 5 min.

Pulse Stimulation and Local Electric Field Modeling

nsPEF exposure of individual cells was performed as described previously (Bowman et al. 2010). Pulses were delivered to a selected group of cells with a pair of custom tungsten rod electrodes (0.08 mm diameter, 0.15 mm gap). Using a robotic micromanipulator (MP-225; Sutter, Novato, CA), electrodes were positioned at 50 μm above the coverslip surface so that the selected cells were located between their tips. Nearly rectangular 60-ns pulses were generated in a transmission line-type circuit, by closing a MOSFET switch upon a timed delivery of a TTL trigger pulse from pClamp software via a Digidata 1322A output (MDS, Foster City, CA). The exact nsPEF delivery protocol and synchronization of nsPEF delivery with image acquisition were programmed in pClamp. The E-field between the electrodes was determined by a 3D simulation with a finite element Maxwell equation solver Amaze 3D (Field Precision, Albuquerque, NM). Exact EP shapes and amplitudes were captured and measured with a Tektronix (Beaverton, OR) TDS 3052 oscilloscope. Experiments included appropriate controls in which cells were subjected to identical manipulations but without nsPEF delivery (“sham” exposures).

Results

The Phenomenon of Pseudopod-Like Blebbing

Pseudopod-like blebbing was discovered when U937 cells were exposed to long trains of nanosecond pulses. PLB formation is illustrated in Fig. 1, which shows representative frames of PLB nucleation and directional growth during exposure to a train of 3,600 60-ns pulses (12.1 kV/cm, 20 Hz).

Bleb formation usually occurs with ~30-s delay after the onset of exposure. After this interval, small rounded blebs appear on the anode-facing cell pole. At this time, these blebs resemble typical blebs widely reported in the literature (Keller et al. 2002; Charras 2008). During the course of treatment, small blebs rapidly elongate toward the anode electrode and may exceed the size of cell diameter after 2 min of exposure. We define such blebs as PLBs. Although the size and growth velocity are distinctive features of PLBs, what makes these blebs unique is that they grow exclusively toward anode and assume an elongated sausage-like appearance. Even blebs nucleated away from anodic cell pole eventually “steer” toward anode. During growth the bleb tip retains its rounded shape and leaves behind the extended bleb body. Developed PLBs commonly have a sectioned appearance due to occasional transverse strictures. When pulse treatment is discontinued, the bleb growth stops promptly and changes to partial or complete retraction.

Role of Pulse Parameters in Triggering Pseudopod-Like Blebbing

For initiation of PLBs we used long trains of 60-ns pulses. At first we focused on the effect of pulse repetition rate and exposure duration while keeping amplitude fixed. Within the tested parameter range, the probability of bleb nucleation was relatively constant and remained at a level of 2–2.5 blebs per cell. However, the probability to form PLBs from regular blebs increased considerably with the increase in pulse rate from 5 to 20 Hz and increase in exposure duration from 30 to 120 s (Fig. 2a). Cells treated with rates of 5, 10 and 20 Hz produced PLBs from 2.9, 10.7 and 28.7 % of regular blebs, respectively. The plot in the right panel of Fig. 2a demonstrates the increase in PLB formation in response to increase in pulse-exposure duration. When other parameters were kept constant, the exposure duration of 30, 60 or 120 s produced 0, 5.4 or 28.7 % of PBLs, respectively.

In the second series of experiments, the E-field was varied from 7.5 to 14.4 kV/cm, while the pulse-repetition rate and exposure duration were fixed at 10 Hz and 120 s, respectively (Fig. 2b). Cell exposure to the lowest tested E-field of 7.5 kV/cm produced a very low regular bleb count of 0.1 blebs/cell and no PLBs. An E-field increase to 9.8 kV/cm resulted in a much higher bleb count of 0.9 blebs/cell but a low relative PLB count (8.7 %). The E-field of 12.1 kV/cm resulted in a bleb count of 1.1 blebs/cell and formation of PLBs from 13.4 % of regular blebs. Exposure to the highest tested E-field of 14.4 kV/cm produced 1.2 blebs/cell, of which 27.7 % were PLBs.

Of note, although two exposure protocols with different frequencies (12.1 kV/cm, 20 Hz, 2,400 pulses in series A and 14.4 kV/cm, 10 Hz, 1,200 pulses in series B) were almost equally efficient at producing PLBs (28.7 and 27.7 %, respectively), we chose the 20-Hz over the 10-Hz protocol for subsequent experiments for the following reasons. First, the velocity of PLB growth at 20 Hz was higher than that at 10 Hz (data not shown). Second, the PLB yield of 10-Hz exposures in series A and B varied, while the PLB yield of the 20-Hz protocol remained steadily high. Based on the studied effects of pulse parameters, selection of 20 Hz seemed the most appropriate due to the maximal yield of PLBs.

Asymmetrical Nucleation of Blebs

In the next series we tested the effect of different pulse protocols on preferred location of bleb nucleation. The cell surface was separated into four sectors relative to position of pulse-delivering electrodes (anodic, cathodic and two sides). All nucleation events were assigned to one of four sectors according to their location. Each bar length in Fig. 3 indicates the percent fraction of nucleation events in the sector to the total number of nucleation events registered for the treatment protocol. In all tested protocols the preferred location of bleb nucleation (~60 %) was at the cell pole facing anode. Other locations displayed a low and nearly equal chance of nucleation. Different bar angles are used merely for convenience of presentation and do not correspond to actual direction of blebbing. Asymmetry of nucleation suggests that permeabilization plays a central role in determining bleb directionality.

Evaluation of Propidium Uptake in Exposed Cells

The propidium emission of nsPEF-treated cells was compared to staining of dead cells which were present in all samples and constituted ~1–2 % of the cell population. The results illustrated in Fig. 4 show that propidium uptake was at least 20-fold lower in nsPEF-exposed cells than in dead cells. This modest uptake level indicates that the membrane barrier function was only partially compromised by nsPEF. However, the long-term viability of PLB-forming cells was not studied.

The Role of Colloid-Osmotic Swelling in PLB Growth

Once the optimal pulse parameters were explored, the mechanisms of PLB growth were addressed. Possible candidates for processes driving bleb formation were electrophoresis, water uptake and cytoskeletal rearrangements. Electrophoretic drift of charged molecules inside the cell is a legitimate expectation during exposure to an electric field; however, a very small duty cycle employed in our treatments (1.2×10^{-6}) renders this unlikely. Presumably, the growth of some cell protrusions is driven by actin polymerization (Chhabra and Higgs 2007), but the growth rate and size of PLBs exceed that of protrusions formed via such mechanism (Pollard and Borisy 2003). Alternatively, PLB growth may be fueled by water uptake. As discussed previously, nsPEF-treated cells swell by a Donnan-type colloid-osmotic mechanism (Pakhomov and Pakhomova 2010; Nesin et al. 2011).

To test the role of the colloid-osmotic mechanism, we partially substituted NaCl for an equiosmolar amount of sucrose, which is a swelling inhibitor in nsPEF-treated cells (Nesin et al. 2011). Exposure buffers in this series contained 45, 90 or 180 mM of sucrose instead of a fraction of NaCl equal to 22.5, 45 or 90 mM, respectively. The results in Fig. 5 illustrate that such replacement is indeed effective against bleb formation. Partial substitution of NaCl for 45 mM of sucrose almost completely eliminated PLBs and modestly affected other bleb types. In the presence of 90 mM of sucrose, no PLBs developed, while formation of other blebs was considerably inhibited. Finally, NaCl replacement for 180 mM of sucrose prevented all types of blebbing. Sham-exposed cells did not produce blebs in any of the buffers.

These results showed that water uptake is indeed the driving mechanism of PLB growth. Thus, formation of both PLBs and regular blebs in nsPEF-treated cells relies on water inflow. However, the elongated shape that contrasts PLBs to regular rounded blebs suggests that other mechanisms, such as cytoskeletal rearrangements, may be involved in PLB formation.

Role of Actin Rearrangements in PLB Formation

In this series we focused on the mechanism responsible for the structural support and shape of PLBs. Considering their monocytic origin, U937 cells may have an advanced regulation of their cytoskeleton (Sheth et al. 1991). As noted above, PLBs commonly extend through the formation of smaller sections that constantly append at the anodic tip. As a result, these blebs commonly have transverse strictures located between two consecutive sections. This observation suggests a complex internal organization of PLBs. We hypothesized that PLB support is provided by formation of an actin scaffold.

In order to establish the role of the actin cytoskeleton, we used a fluorescent rhodamine-phalloidin conjugate. Conveniently, nsPEF treatment improved penetration of the conjugate inside the cell and enabled efficient actin visualization at a low dye concentration. The time series of DIC and corresponding actin staining images during PLB development are presented in Fig. 6a. PLB growth was accompanied by the accumulation of actin in the bleb interior. After nsPEF exposure, bleb growth stopped and concurrently the formation of an actin rim began along the bleb surface. The assembly of the actin cortex preceded partial PLB retraction. During the retraction, PLBs deflated and assumed a wrinkled appearance that corresponded to intense actin accumulation in the bleb body.

To verify the role of actin in support of the PLB shape, we inhibited actin polymerization by the addition of cytochalasin D (1 nM). The results in Fig. 6b show that in the presence of cytochalasin D nsPEF exposure induced formation of regular rounded blebs rather than PLBs. After pulse treatment, rounded blebs did not retract or develop an actin rim.

Overall, the inhibition of F-actin formation by cytochalasin D prevented formation of PLBs. Together with fluorescent labeling data, this demonstrates that actin polymerization is responsible for the unique PLB shape and its retraction.

In summary, we established that the driving force of PLB growth was Donnan-type colloid-osmotic water uptake, while the specific bleb shape arises due to formation of the actin cytoskeleton.

Discussion

The experiments above clearly define pseudopod-like blebbing as a phenomenon different from both apoptotic and necrotic blebbing, which are commonly associated with electric pulse exposure. PLBs exhibit distinctive features, like elongated shape and growth directionality, and to our best knowledge have not been reported previously. Whether PLBs are exclusive to nsPEF or can also be produced by longer pulses remains to be established.

PLBs form predominantly on the anode-facing cell surface during exposure to long trains of nanosecond pulses. During pulse application, the anodic pole is subject to the largest induced transmembrane voltage and most intense permeabilization (Frey et al. 2006; White et al. 2011). Prolonged permeabilization is an essential prerequisite for PLB formation. Water uptake in the permeabilized area driven by the colloid-osmotic gradient is the primary force for PLB nucleation and growth. Although water uptake starts immediately after permeabilization, PLB formation typically begins in about 30 s. We propose that this interval is required for water uptake and the corresponding increase in intracellular pressure that would result in bleb nucleation. Alternatively, based on the poroelastic cell concept (Charras et al. 2009), a 30-s interval may be required for buildup of the pressure locally. According to this hypothesis, the increase in local pressure may result from a slow pressure equilibration across the whole cell. In addition, we do not exclude the possibility of a direct impact of membrane depolarization or pulse damage on membrane–cytoskeleton interactions.

The growth of PLBs occurs exclusively during nsPEF treatment and is directed toward the anode electrode. Prolonged nsPEF treatment results in continual permeabilization on the anodic pole and formation of a bleb tip that migrates toward anode concurrently with bleb elongation. Continual permeabilization of the tip generates constant influx of extracellular water and determines the direction of extension. According to this assumption, the anodotropic direction of PLB growth is not an effect of the electric field but rather a result of constant permeabilization of the anodic cell pole.

Although we demonstrated that the colloid-osmotic gradient is the driving mechanism of PBL extension, this does not explain the characteristic elongated shape of PLBs. We established that bleb elongation is accompanied by formation of an actin cytoskeleton in the bleb interior. Supposedly, prompt recruitment of actin into the bleb reinforces bleb walls and prevents bleb growth sideways. Meanwhile, continual permeabilization on the anodic pole promotes bleb growth toward the electrode. Polymerization of actin coupled with continual bleb formation at the growing tip may also be responsible for the sectioned PLB appearance. Blockage of actin polymerization permits bleb spreading in all directions, thereby inhibiting PLBs and resulting in the formation of stationary rounded blebs with no retraction capability. Such blebs are morphologically indistinguishable from terminal blebs formed in necrotic cells. Formation of the actin scaffold culminates in assembly of the bleb cortex and is responsible for PLB retraction when the exposure ends. Actin assembly and retraction of PLBs is an active process, suggesting that nsPEF treatment does not damage cells beyond their repair capacity. This assumption combined with a modest level of propidium uptake

suggests that PLB formation is hardly a manifestation of cell necrosis. More likely such nsPEF-guided protrusive blebbing provides a mechanism to expand and retract the cell membrane in a controlled manner.

Protrusion formation is an essential part of cell migration (Bereiter-Hahn 2005). Accumulating evidence suggests that during protrusion formation, contrary to the traditional view (Pollard and Borisy 2003), water inflow (Loitto et al. 2002) and membrane evagination precede actin assembly (Yang et al. 2009) and not the opposite. Our experiments established that inhibition of water uptake is sufficient to inhibit nucleation of PLBs and other blebs, while inhibition of actin polymerization does not prevent nucleation. In view of these findings, it may be interesting to examine the role of water uptake in other types of cell protrusions. However, the relevance of pseudopod-like blebbing to cell protrusions in general, including blebbing associated with cell motility, remains to be established.

Within the range of tested pulse conditions, PLB formation was observed in U937 cells but not in several other cell types (CHO, Jurkat and GH3; data not presented here). This may indicate the lack of free actin monomers in these cells or suboptimal nsPEF treatment conditions. Although PLBs may be specific to a particular cell type, they may provide a valuable model for investigation of blebbing and other protrusions. Fast initiation, high yield and flexible control over pulse-exposure parameters make this phenomenon easy to manage. Further investigation of PLBs may provide insights into membrane trafficking, cytoskeletal rearrangements and transmembrane water transport not only in electroporated cells but also in cells studied in their physiological environment.

Acknowledgments

The work was funded by R01CA125482 from the National Cancer Institute and R01GM088303 from the National Institute of General Medical Sciences.

References

André FM, Rassokhin MA, Bowman AM, Pakhomov AG. Gadolinium blocks membrane permeabilization induced by nanosecond electric pulses and reduces cell death. Bioelectrochemistry. 2010; 79(1):95–100. [PubMed: 20097138]

Barros LF, Kanaseki T, Sabirov R, Morishima S, Castro J, Bittner CX, Maeno E, Ando-Akatsuka Y, Okada Y. Apoptotic and necrotic blebs in epithelial cells display similar neck diameters but different kinase dependency. Cell Death Differ. 2003; 10(6):687–697. [PubMed: 12761577]

Bereiter-Hahn J. Mechanics of crawling cells. Med Eng Phys. 2005; 27(9):743–753. [PubMed: 15963752]

Bereiter-Hahn J, Luck M, Miebach T, Stelzer HK, Voth M. Spreading of trypsinized cells: cytoskeletal dynamics and energy requirements. J Cell Sci. 1990; 96(1):171–188. [PubMed: 2373741]

Blaser H, Reichman-Fried M, Castanon I, Dumstrei K, Marlow FL, Kawakami K, Solnica-Krezel L, Heisenberg CP, Raz E. Migration of zebrafish primordial germ cells: a role for myosin contraction and cytoplasmic flow. Dev Cell. 2006; 11(5):613–627. [PubMed: 17084355]

Bowman A, Nesin O, Pakhomova O, Pakhomov A. Analysis of plasma membrane integrity by fluorescent detection of Tl^+ uptake. J Membr Biol. 2010; 236(1):15–26. [PubMed: 20623351]

Charras GT. A short history of blebbing. J Microsc. 2008; 231(3):466–478. [PubMed: 18755002]

Charras G, Paluch E. Blebs lead the way: how to migrate without lamellipodia. Nat Rev Mol Cell Biol. 2008; 9(9):730–736. [PubMed: 18628785]

Charras GT, Yarrow JC, Horton MA, Mahadevan L, Mitchison TJ. Non-equilibration of hydrostatic pressure in blebbing cells. Nature. 2005; 435(7040):365–369. [PubMed: 15902261]

Charras GT, Hu C-K, Coughlin M, Mitchison TJ. Reassembly of contractile actin cortex in cell blebs. J Cell Biol. 2006; 175(3):477–490. [PubMed: 17088428]

Charras GT, Mitchison TJ, Mahadevan L. Animal cell hydraulics. J Cell Sci. 2009; 122(18):3233–3241. [PubMed: 19690051]

Chhabra ES, Higgs HN. The many faces of actin: matching assembly factors with cellular structures. Nat Cell Biol. 2007; 9(10):1110–1121. [PubMed: 17909522]

Cunningham CC. Actin polymerization and intracellular solvent flow in cell surface blebbing. J Cell Biol. 1995; 129(6):1589–1599. [PubMed: 7790356]

Cunningham CC, Gorlin JB, Kwiatkowski DJ, Hartwig JH, Janmey PA, Byers HR, Stossel TP. Actin-binding protein requirement for cortical stability and efficient locomotion. Science. 1992; 255(5042):325–327. [PubMed: 1549777]

Dai J, Sheetz MP. Membrane tether formation from blebbing cells. Biophys J. 1999; 77(6):3363–3370. [PubMed: 10585959]

Deng J, Schoenbach KH, Stephen Buescher E, Hair PS, Fox PM, Beebe SJ. The effects of intense submicrosecond electrical pulses on cells. Biophys J. 2003; 84(4):2709–2714. [PubMed: 12668479]

Derivery E, Fink J, Martin D, Houdusse A, Piel M, Stradal TE, Louvard D, Gautreau A. Free brick1 is a trimeric precursor in the assembly of a functional wave complex. PLoS ONE. 2008; 3(6):e2462. [PubMed: 18560548]

Fackler OT, Grosse R. Cell motility through plasma membrane blebbing. J Cell Biol. 2008; 181(6): 879–884. [PubMed: 18541702]

Frey W, White JA, Price RO, Blackmore PF, Joshi RP, Nuccitelli R, Beebe SJ, Schoenbach KH, Kolb JF. Plasma membrane voltage changes during nanosecond pulsed electric field exposure. Biophys J. 2006; 90(10):3608–3615. [PubMed: 16513782]

Gass GV, Chernomordik LV. Reversible large-scale deformations in the membranes of electrically-treated cells: electroinduced bleb formation. Biochim Biophys Acta. 1990; 1023(1):1–11. [PubMed: 2317489]

Hoffmann EK, Lambert IH, Pedersen SF. Physiology of cell volume regulation in vertebrates. Physiol Rev. 2009; 89(1):193–277. [PubMed: 19126758]

Hogue MJ. The effect of hypotonic and hypertonic solutions on fibroblasts of the embryonic chick heart in vitro. J Exp Med. 1919; 30(6):617–648. [PubMed: 19868382]

Holtfreter J. A study of the mechanics of gastrulation. J Exp Zool. 1944; 95(2):171–212.

Keller H, Eggli P. Protrusive activity, cytoplasmic compartmentalization, and restriction rings in locomoting blebbing Walker carcinosarcoma cells are related to detachment of cortical actin from the plasma membrane. Cell Motil Cytoskelet. 1998; 41(2):181–193.

Keller H, Rentsch P, Hagmann J. Differences in cortical actin structure and dynamics document that different types of blebs are formed by distinct mechanisms. Exp Cell Res. 2002; 277(2):161–172. [PubMed: 12083798]

Kinosita K Jr, Tsong TT. Hemolysis of human erythrocytes by transient electric field. Proc Natl Acad Sci USA. 1977; 74(5):1923–1927. [PubMed: 266714]

Lang TU, Khalbuss WE, Monaco SE, Michelow P, Pantanowitz L. Review of HIV-related cytopathology. Pathol Res Int. 2011; 2011 256083.

Loitto V-M, Forslund T, Sundqvist T, Magnusson K-E, Gustafsson M. Neutrophil leukocyte motility requires directed water influx. J Leukocyte Biol. 2002; 71(2):212–222. [PubMed: 11818441]

Maugis B, Brugues J, Nassoy P, Guillen N, Sens P, Amblard F. Dynamic instability of the intracellular pressure drives bleb-based motility. J Cell Sci. 2010; 123(22):3884–3892. [PubMed: 20980385]

Mitchison TJ, Charras GT, Mahadevan L. Implications of a poroelastic cytoplasm for the dynamics of animal cell shape. Semin Cell Dev Biol. 2008; 19(3):215–223. [PubMed: 18395478]

Nesin OM, Pakhomova ON, Xiao S, Pakhomov AG. Manipulation of cell volume and membrane pore comparison following single cell permeabilization with 60- and 600-ns electric pulses. Biochim Biophys Acta. 2011; 1808(3):792–801. [PubMed: 21182825]

Norman L, Sengupta K, Aranda-Espinoza H. Blebbing dynamics during endothelial cell spreading. Eur J Cell Biol. 2011; 90(1):37–48. [PubMed: 21087809]

Pakhomov, AG.; Pakhomova, ON. Nanopores: a distinct transmembrane passageway in electroporated cells. In: Pakhomov, AG.; Miklavcic, D.; Markov, MS., editors. Advanced electroporation techniques in biology and medicine. Boca Raton: CRC Press; 2010. p. 178-194.

Pakhomov AG, Bowman AM, Ibey BL, Andre FM, Pakhomova ON, Schoenbach KH. Lipid nanopores can form a stable, ion channel-like conduction pathway in cell membrane. Biochem Biophys Res Commun. 2009; 385(2):181–186. [PubMed: 19450553]

Petersen MA, Dailey ME. Diverse microglial motility behaviors during clearance of dead cells in hippocampal slices. Glia. 2004; 46(2):195–206. [PubMed: 15042586]

Pletjushkina OJ, Rajfur Z, Pomorski P, Oliver TN, Vasiliev JM, Jacobson KA. Induction of cortical oscillations in spreading cells by depolymerization of microtubules. Cell Motil Cytoskelet. 2001; 48(4):235–244.

Pollard TD, Borisy GG. Cellular motility driven by assembly and disassembly of actin filaments. Cell. 2003; 112(4):453–465. [PubMed: 12600310]

Rassokhin, MA.; Pakhomov, AG. Fast anodotropic expansion of cell membrane under exposure to high-rate nanosecond duration electric pulses (nsEP). The American society for cell biology 50th annual meeting; December 2010; Philadelphia, PA, USA. 2010. p. 11-15.

Rassokhin, MA.; Pakhomov, AG. Cell reshaping triggered by nanosecond electric pulses (nsEP). 8th international bioelectrics symposium; May 2011; Toulouse, France. 2011. p. 4-6.

Saulis G. Cell electroporation: estimation of the number of pores and their sizes. Biomed Sci Instrum. 1999; 35:291–296. [PubMed: 11143365]

Sebbagh M, Renvoize C, Hamelin J, Riche N, Bertoglio J, Breard J. Caspase-3-mediated cleavage of ROCK I induces MLC phosphorylation and apoptotic membrane blebbing. Nat Cell Biol. 2001; 3(4):346–352. [PubMed: 11283607]

Sheth B, Banks P, Burton DR, Monk PN. The regulation of actin polymerization in differentiating U937 cells correlates with increased membrane levels of the pertussis-toxin-sensitive G-protein Gi2. Biochem J. 1991; 275(Pt 3):809–811. [PubMed: 1645523]

Tekle E, Wolfe MD, Oubrahim H, Chock PB. Phagocytic clearance of electric field induced “apoptosis-mimetic” cells. Biochem Biophys Res Commun. 2008; 376(2):256–260. [PubMed: 18771656]

Tinevez J-Y, Schulze U, Salbreux G, Roensch J, Joanny J-F, Paluch E. Role of cortical tension in bleb growth. Proc Natl Acad Sci. 2009; 106(44):18581–18586. [PubMed: 19846787]

Torgerson RR, McNiven MA. The actin-myosin cytoskeleton mediates reversible agonist-induced membrane blebbing. J Cell Sci. 1998; 111(19):2911–2922. [PubMed: 9730983]

Tsong TY. Electroporation of cell membranes. Biophys J. 1991; 60(2):297–306. [PubMed: 1912274]

White J, Pliquett U, Blackmore P, Joshi R, Schoenbach K, Kolb J. Plasma membrane charging of Jurkat cells by nanosecond pulsed electric fields. Eur Biophys J. 2011; 40(8):947–957. [PubMed: 21594746]

Yang C, Hoelzle M, Disanza A, Scita G, Svitkina T. Coordination of membrane and actin cytoskeleton dynamics during filopodia protrusion. PLoS ONE. 2009; 4(5):e5678. [PubMed: 19479071]

Zollinger HU. Cytologic studies with the phase microscope; morphologic changes associated with the death of cells in vitro and in vivo. Am J Pathol. 1948; 24(5):1039–1053. [PubMed: 18883952]

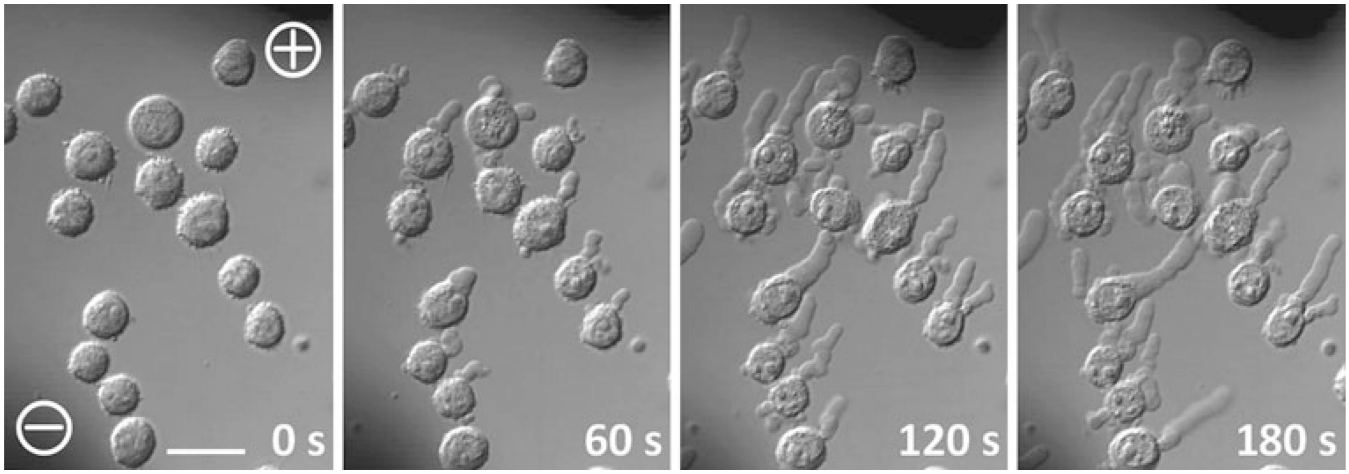

Fig. 1.

Nanosecond pulsed electric field (nsPEF) exposure triggers and guides formation of anodotropic pseudopod-like blebs. Images show representative frames of time series illustrating U937 cells at different time points (60-s interval) during exposure to 60-ns pulses (12.1 kV/cm, 20 Hz, 3,600 pulses). Pulse treatment started at 0 s. Shadows at the *upper right* and *lower left* corners are those of nsPEF-delivering electrodes. Anode and cathode electrodes are identified by + and − signs, respectively. *Scale bar* = 20 μm

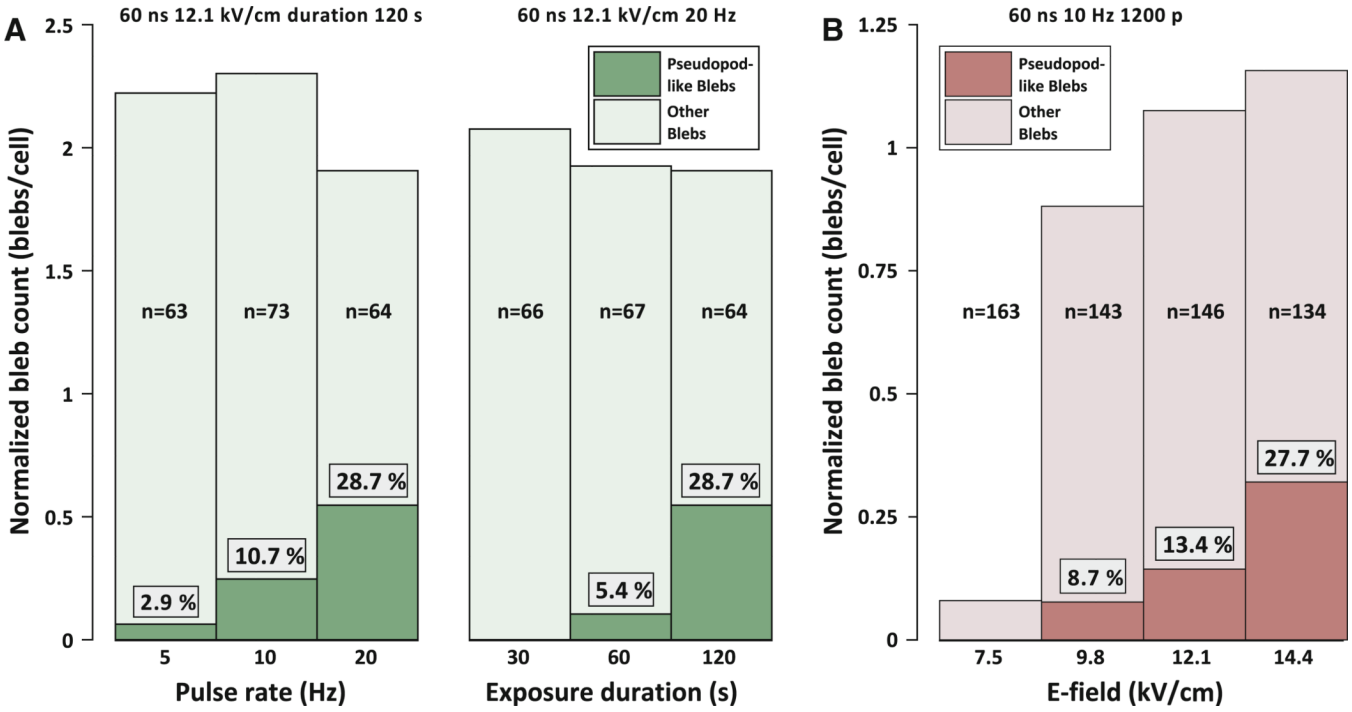

Fig. 2.

Effect of the treatment parameters on formation of regular and pseudopod-like blebs. *Numbers* on the graphs indicate the number of analyzed cells and the percentage of pseudopod-like blebs in the overall bleb count. The set of parameters indicated above each chart was kept constant, while parameters below the charts were varied. **a** *Left panel* Pulse rate was varied while keeping other parameters constant. *Right panel* Exposure duration was varied while keeping other parameters constant. One group (20 Hz, 2,400 pulses) is shared between the two charts. **b** E-field was varied while all other parameters were constant. Plots **a** and **b** summarize the results of 8 and 15 independent treatments, respectively. Sham-exposed cells did not produce any blebs (not shown)

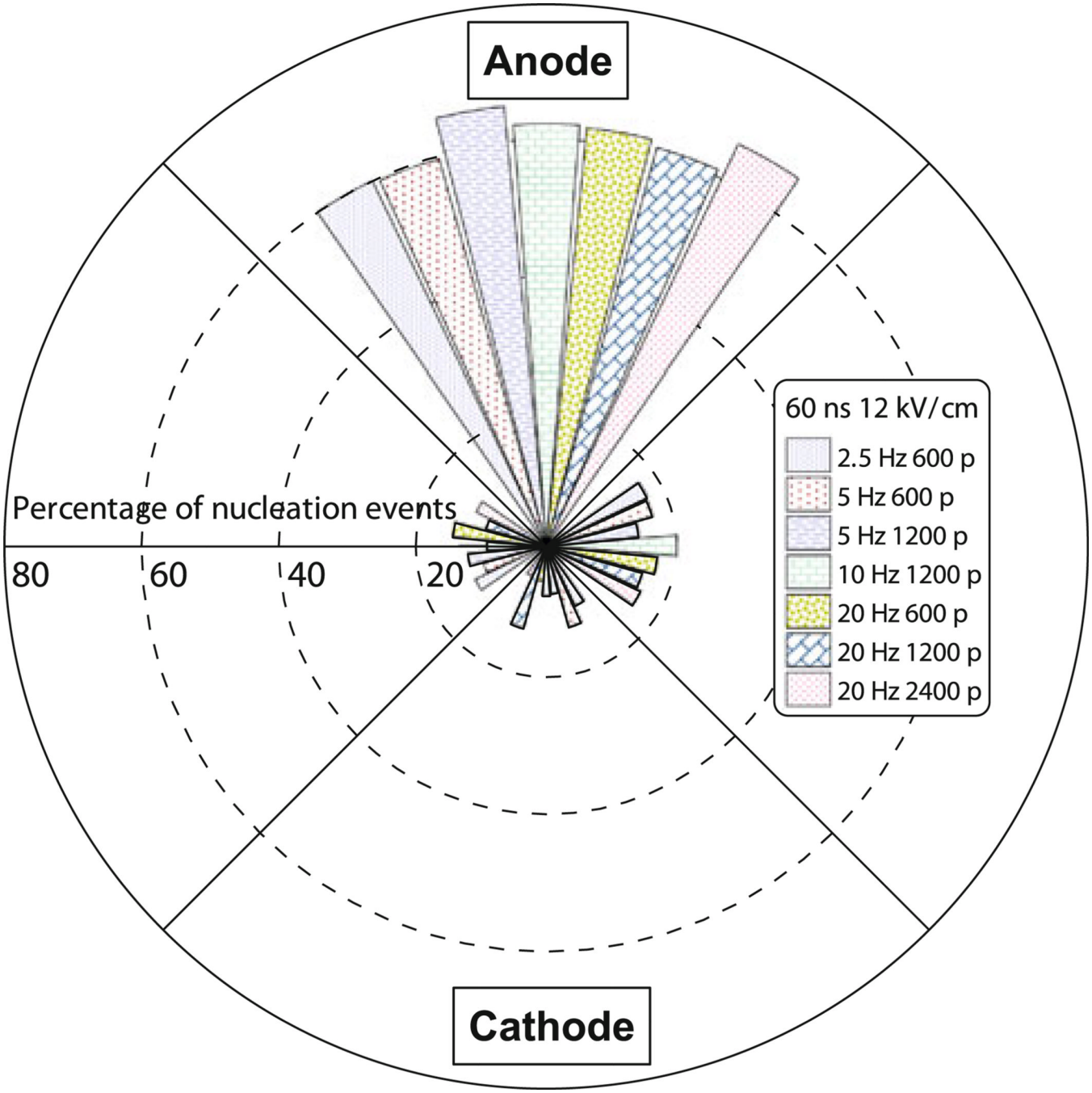

Fig. 3.

Blebs are predominantly nucleated at the anodic cell pole. Bleb initiation was evaluated during exposure to one of the pulse protocols shown in the graph. For each treatment the number of nucleation events was measured in four 90° sectors of the cell surface (anodic, cathodic and two sides). The total number of nucleation events in each protocol was taken for 100 %. *Bars* encode the fraction of nucleation events and do not imply exact bleb position against the electrodes. Data summarize the results of eight experiments for each protocol

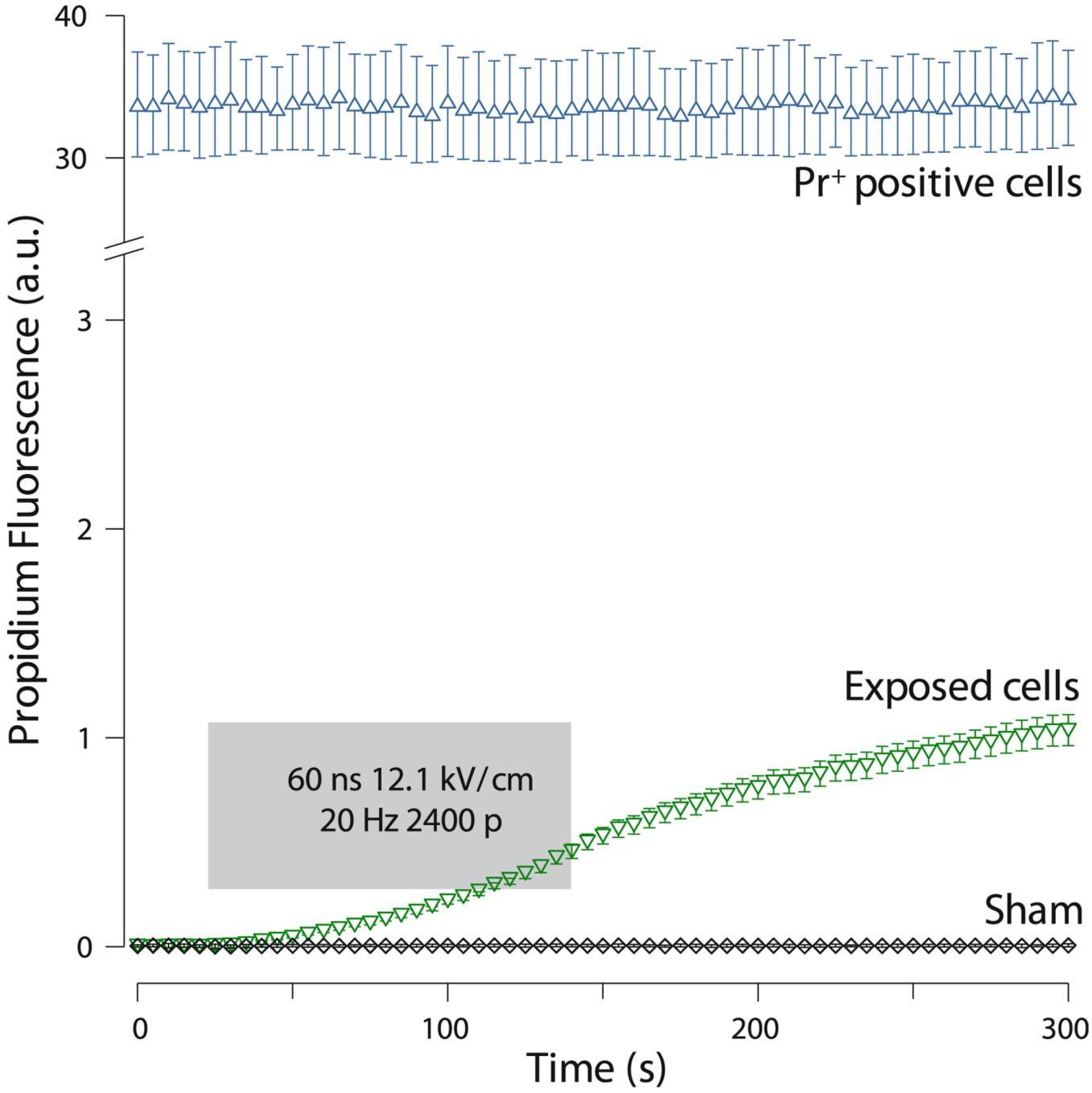

Fig. 4.

Nanosecond pulsed electric field–triggered propidium uptake compared to uptake in sham-exposure cells and dead cells. Dead cells typically constitute ~1–2 % of cell samples. Shading represents the exposure interval. Note the scale break on the fluorescence axis. The exposed group presents recordings of 53 cells in eight independent experiments

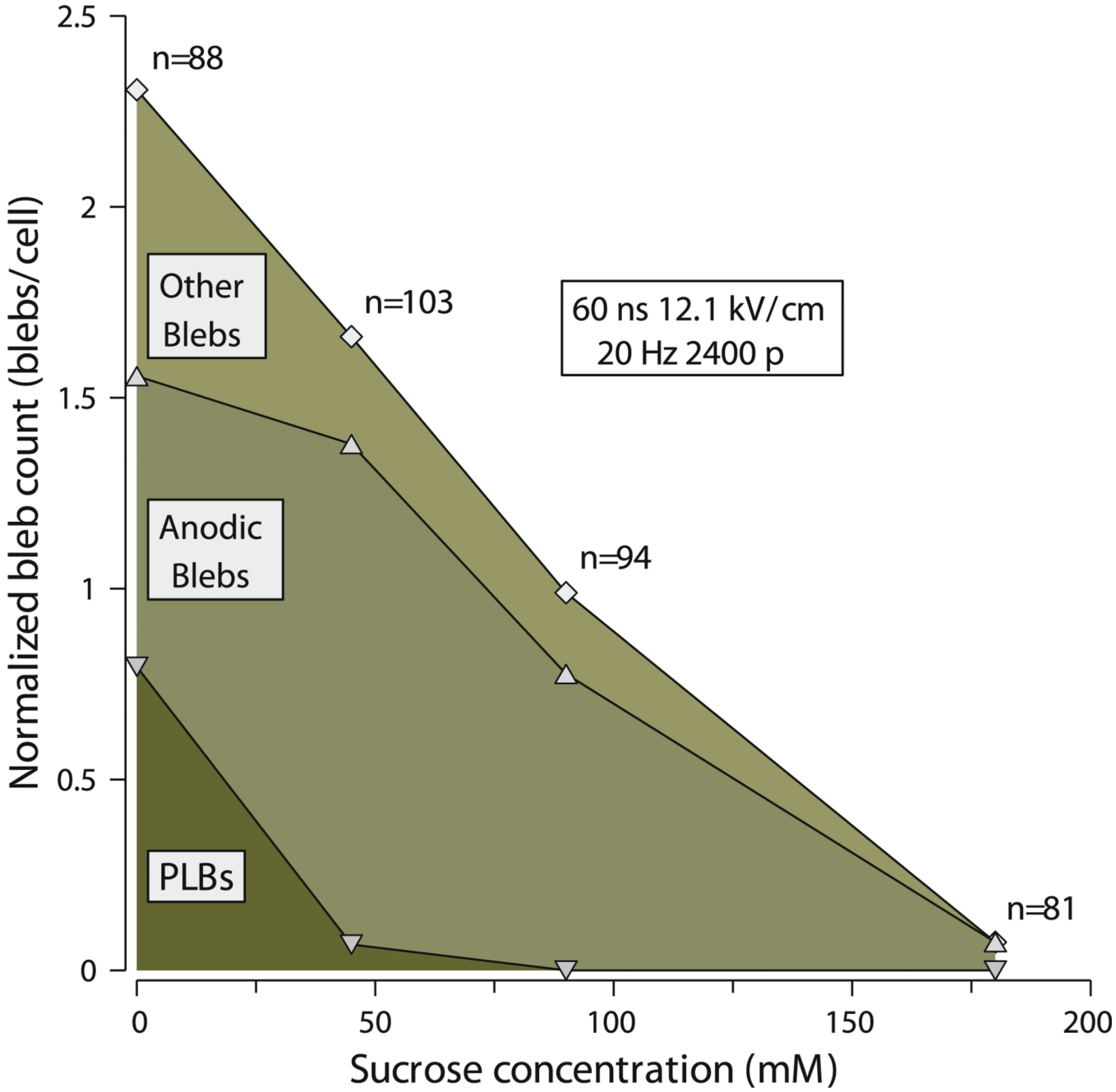

Fig. 5.

Inhibition of nanosecond pulsed electric field–induced blebbing by isosmotic replacement of different fractions of NaCl for sucrose. Replacement of equiosmolar amount of NaCl for sucrose inhibits water uptake by electroporated cells and does not change the final buffer osmolality. The number of blebs per cell was plotted against the fraction of sucrose in the buffer (45, 90 and 180 mM). The cell count is the sum of eight independent experiments

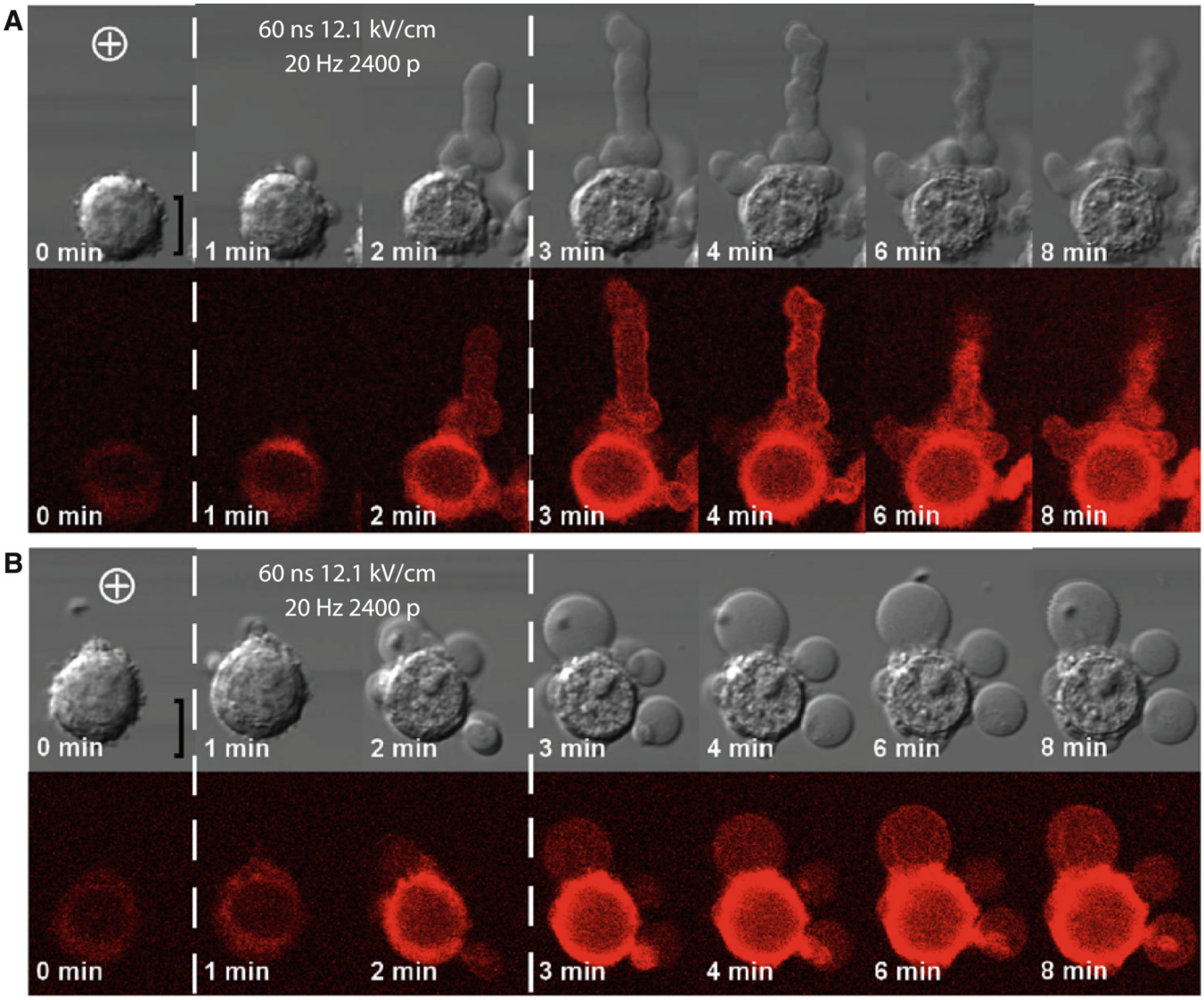

Fig. 6.

Cytoskeleton formation in pseudopod-like blebs (PLBs) and the effect of F-actin inhibition on bleb shape and retraction. Representative frames of an image time series demonstrate blebs in U937 cells before, during and after nanosecond pulsed electric field treatment (started at 30 s). Pseudopod-like blebbing (**a**) is accompanied by formation of an actin rim and partial bleb retraction after exposure. The presence of cytochalasin D (**b**) inhibits PLB formation. Rounded blebs that form instead do not develop the actin rim and lack the retraction capability. *Dashed lines* enclose frames recorded during exposure. *Scale bar* = 10 μm